Correction of gradient echo images for first and second order macroscopic signal dephasing using phase derivative mapping

Hendrik de Leeuw[1], and Chris J.G. Bakker[1]
[1]*Image Sciences Institute, Utrecht, Utrecht, Netherlands*

Introduction: Gradient Echo (GE) MR imaging is routinely used for many purposes [1-2]. The choice for GE is usually governed by its sensitivity for mesoscopic field inhomogeneities, which characterizes susceptibility differences within tissue [3, 4]. GE, however, is hampered by macroscopic field inhomogeneities which extend beyond the voxel level, such as inhomogeneities invoked by air cavities. Three categories of methods have been proposed to reduce macroscopic signal dephasing effects. First, methods in which the signal acquisitions itself is adapted. These methods require precise tuning of the scan parameters and lack flexibility or lengthen the scan duration [2, 5-7]. Second, methods in which the signal reconstruction is exploited to reduce effects of macroscopic signal dephasing. To allow for this compensation of macroscopic signal dephasing, the reconstruction methods require additional acquisitions and lengthen the reconstruction duration significantly [4, 8, 9]. The third solution encompasses methods that incorporate the macroscopic signal dephasing into the model used for fitting the data. These methods can be applied to multi-echo data only and can, for increasingly sophisticated models, end up in a local minimum [10, 11]. Herein, a generally applicable post-processing method is presented which compensates for signal alterations invoked by first and second order macroscopic phase incoherences, while leaving mesoscopic effect unperturbed. The method is demonstrated for a phantom containing paramagnetic particles and the head of a volunteer, respectively.

Theory: The signal (s) in a voxel at location (x_0) is given by an integral over the isochromats within that voxel, with signal phase (φ) and an effective spin density ρ that incorporates (T_1-, T_2-) relaxation effects.

$$s[x_0] = \int_{voxel} dx\, \rho[x] \cdot \exp[i\varphi[x]] \qquad (1)$$

Using a Taylor expansion of the signal phase about $x=x_0$ and a constant ρ, the acquired signal can be rewritten:

$$s[x_0] = s_0[x_0] \cdot \int_{voxel} dx \exp[i(\varphi_0[x_0] + \frac{\partial\varphi}{\partial x}[x_0] \cdot x + \frac{1}{2}\partial^2\varphi / \partial x^2 [x_0] \cdot x^2)] \qquad (2)$$

Hence, the acquired signal can be written in terms of the unperturbed signal of a voxel times a dephasing term. Evaluating the integral up to the first or second order Taylor expansion gives expressions for first and second order signal dephasing terms, respectively [10,11]. Phase derivatives were obtained as described earlier [12].

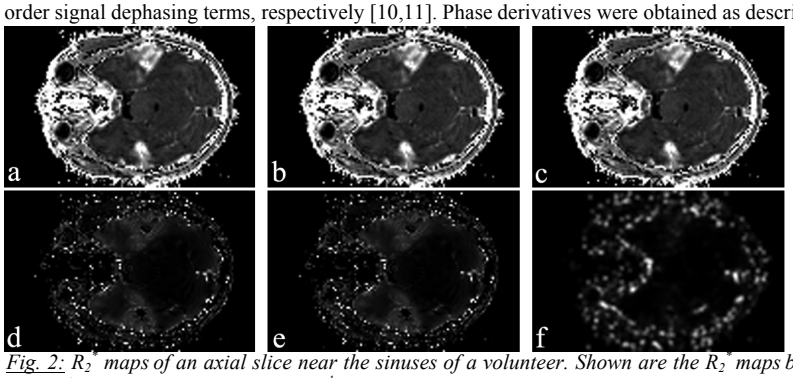

Fig. 2: R_2^* maps of an axial slice near the sinuses of a volunteer. Shown are the R_2^* maps before correction, after 1st order correction and after 2nd order correction (Fig a, b and c respectively). The bottom row depicts the difference in R_2^* between 1st order corrected and uncorrected data (d), between 2nd order corrected and uncorrected data (e) and between 2nd and 1st order corrected data (f). Image scale is rendered on the right.

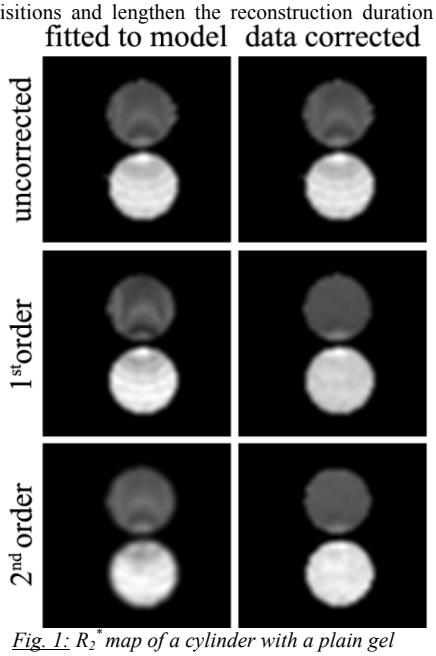

Fig. 1: R_2^* map of a cylinder with a plain gel (top) and a cylinder with a gel containing Holmium loaded microspheres representing mesoscopic field disturbers (bottom). The right column presents the R_2^* maps obtained by fitting to a mono-exponential model after correction of the data for 1st or 2nd order macroscopic signal dephasing, the left column shows the R_2^* maps obtained by fitting the data to a model that includes 1st and 2nd order signal dephasing.

Materials & Methods: Phantom experiments were performed with a phantom consisting of two cylinders viz. a cylinder containing a 2% agar gel with 30mg/L $MnCl_2$ and a cylinder with the same gel in which 4mg/ml of Holmium loaded microspheres (18.6% w/w Holmium, 30µm diameter) were dispersed [1]. In-vivo studies were performed on the brain of a 27-year old female volunteer. Imaging was done on a 1.5T clinical whole body MR system (Achieva 1.5T, Philips Medical Systems, Best, The Netherlands). A velocity compensated, RF spoiled GE sequence (16 echoes) was applied. For the phantom scan parameters included FOV 64^3 mm^3, matrix 64^2x32, TR 39ms, TE_1 2.3ms, ΔTE 2.3ms, θ 15°, NEX 1 and read-out BW 856 Hz, resulting in a scan duration of 1.04min. Scan parameter for the volunteer study included FOV 256^2x164 mm^3, matrix 128^2x82, TR 55ms, TE_1 2.6ms, ΔTE 4.6ms, θ 25°, NEX 1 and read-out BW 1.17 kHz (volunteer), resulting in scan duration of 9.35min.

Data was processed with in-house developed software written in Matlab (Mathworks, Natick, MA). To calculate the total signal perturbation, the perturbation along each direction (Eq.1) was multiplied. Correction was performed by dividing the acquired data by the calculated signal perturbation. First order correction and the second order correction were incorporated in a non-linear least-square fitting routine using a Levenberg-Marquardt algorithm [11, 12]. All processing was done using a homebuilt image processing environment. Typical processing time for the correction model on a 3D dataset of 64x64x32x16 elements was 5min, fitting of the L-M models required 60 min. Fitting to the exponential model was performed by a linearization of the fitting model and required 5sec [13].

Results & Discussion: Fig. 1 shows the result of the phantom experiments. The paramagnetic Holmium loaded microspheres result in a mesoscopic effect on the signal, resulting in an increased R_2^* [1]. For both gels, the macroscopic magnetic field of one perturbs the macroscopic magnetic field of the other. This is shown to induce an increase of the R_2^* near the interface of the two cylinders. The results for the R_2^* are improved more by 2nd order correction (bottom row) than by 1st order correction (middle row). Correcting the data before fitting (right column) turns out to be more stable than fitting with a model that includes the signal dephasing models (left column) and shows less variation of the R_2^* over the whole cylinder (not shown). This suggests that macroscopic signal dephasing effects are reduced, while mesoscopic effects are left unperturbed. Locally a small increase of the R_2^* is still observed after correction. This is caused by a strongly varying magnetic field, which requires higher than 2nd order expansion and correction and results in image distortion. Image distortion can, amongst others, be minimized by acquiring data with a strong read-out gradient [14]. The influence of the correction on the R_2^* in-vivo is presented in Fig. 2. The corrections affect the R_2^* throughout the whole brain and display a substantial correction near the sinuses. The corrections of R_2^* are generally relatively small ($\approx 0.2 s^{-1}$), except near the air tissue interfaces, where corrections of the order of 1-3 s^{-1} are observed. Multiple slices are seen to be affected by the correction and hence were affected by signal loss. The correction ($2 s^{-1}$) is of the same order of magnitude as found by others [10]. The changes on R_2^* imposed by the 2nd order corrections are minor ($\leq 0.2 s^{-1}$) and are primarily located near interfaces. Since the method uses the acquired data only, the method can be applied to single as well as multi-echo data. Furthermore, the method only corrects for dephasing present in the data and, since the fitting involves a single exponential, it will not end up in a local minimum.

References: [1] J.H. Seppenwoolde et al. *MRM*, 53(1):76–84, 2005. [2] R.J. Ordidge et al. *MRM*, 32(3):335–341,1994. [3] S. Baudrexel et al. *MRM,* 62(1):263–268, 2009.[4] S.Volz et al. *NeuroImage*, 45(4):1135–1143, 2009. [5] S. Posse et al. *NeuroImage*, 18(2): 390–400, 2003. [6] J.H. Seppenwoolde et al. *MRM*, 50(4):784–790, 2003 [7] M. Stuber et al. *MRM*, 58(5):1072–1077, 2007. [8] H Schomberg. *IEEE TMI*, 18(6):481–495,1999. [9] T. Knopp et al. *IEEE TMI*, 28(3):394–404, 2009.[10] M.A. Fernandez et al.*MRM*, 44(3):358–366,2000.[11] X.Yang et al. *MRM*,63(5):1258–1268,2010.[12]H. de Leeuw et al. *Proc. ISMRM: 261,*2009.[13] E.W. Weisstein. http://mathworld.wolfram.com /LeastSquaresFittingExponential.html.[14] N.K. Chen et al.*Neuroimage,*19(3):817–825,2003